Supplementary Figures

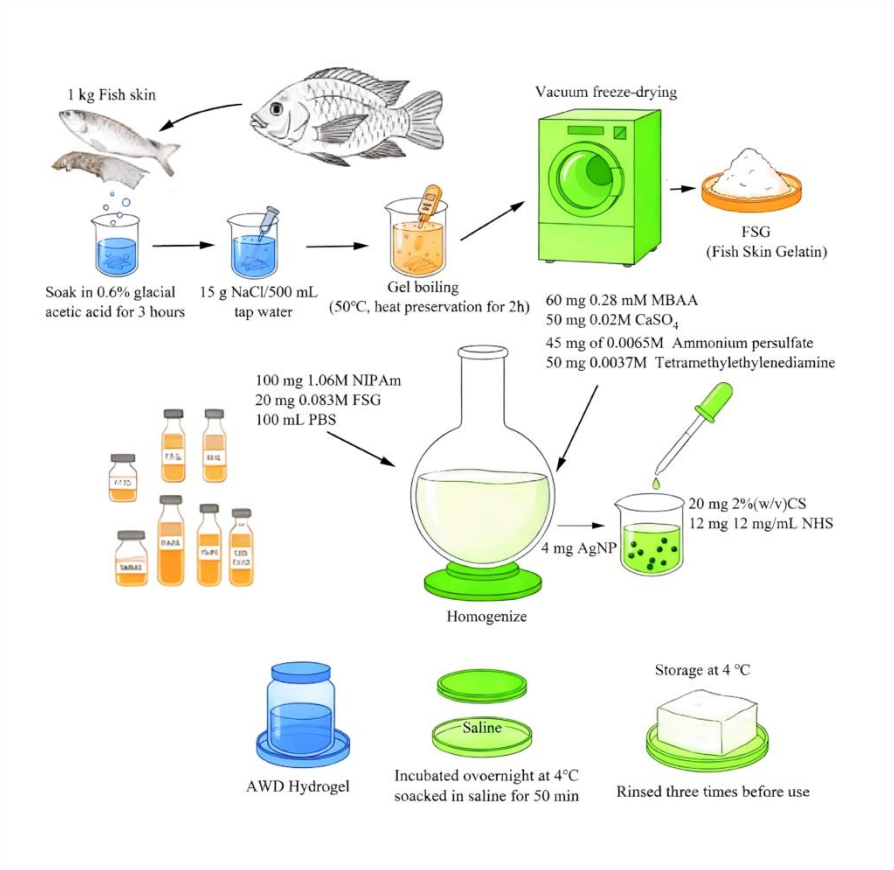

Supplementary Figure S1 Schematic diagram of AWD preparation process

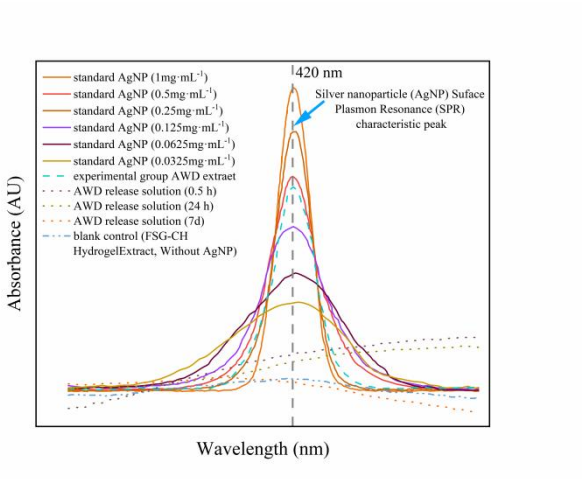

Supplementary Figure S2 UV-Vis absorption spectra of AgNP surface plasmon resonance (SPR) characteristics: standard AgNP solutions, AWD extracts, and release solutions.

(a) (b)

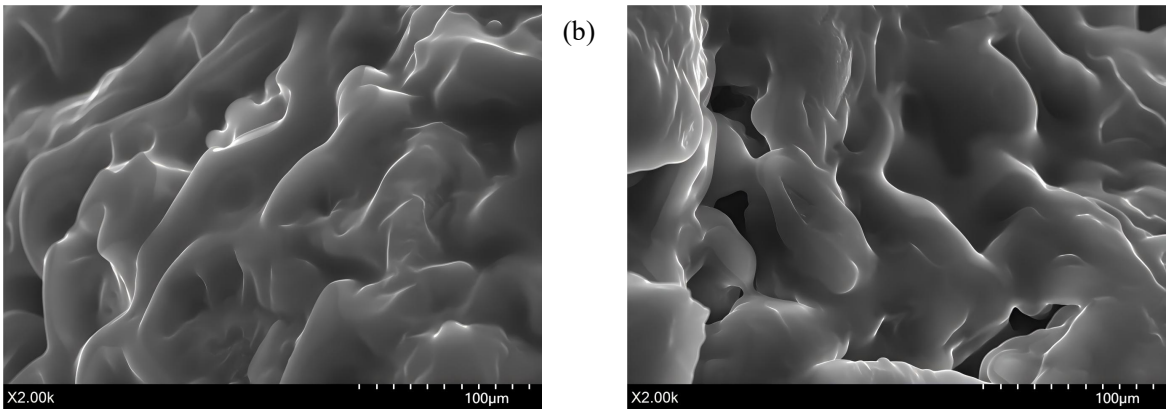

Supplementary Figure S3 Representative FE-SEM images of AWD (a) and OAWD (b) (scale bar: 100 µm)

FSG, CS, PNIPAm, OAWD and AWD samples were directly placed on the ATR crystal of the FTIR spectrometer (Nicolet iS50, Thermo Fisher Scientific, USA) to ensure tight contact. The scanning range was set to 4000–400 cm^{-1} with 32 scans and a resolution of 4 cm^{-1}. Air was used as the background for baseline correction, and infrared spectra were recorded. The chemical structure and crosslinking interactions were analyzed based on the position, intensity, and shift of characteristic peaks.

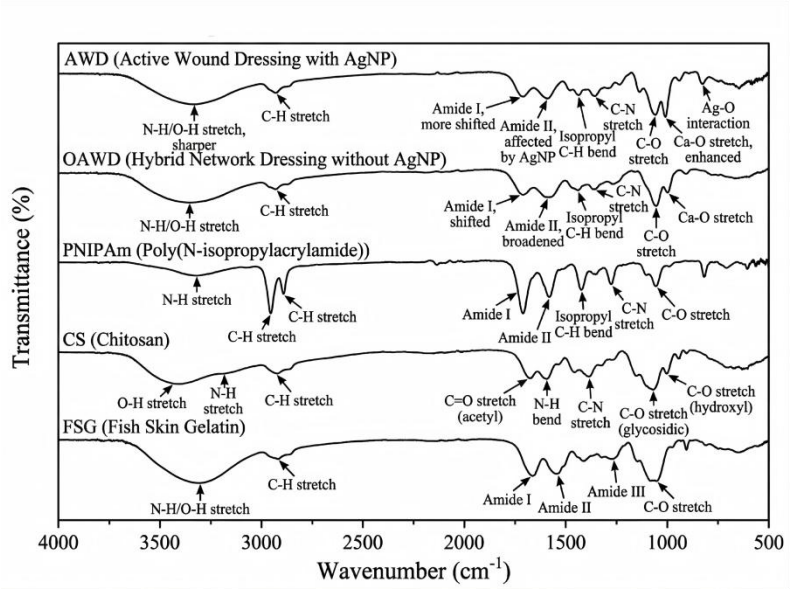

Supplementary Figure S4 Comparative FTIR spectra of AWD, OAWD, PNIPAm, CS, and FSG

DSC Analysis: 5–8 mg of AWD sample was sealed in an aluminum pan, with an empty aluminum pan as the reference. The sample was heated from 0°C to 80°C at a rate of 10°C·min^{-1} under a nitrogen atmosphere (flow rate: 50 mL·min^{-1}. The lower critical solution temperature (LCST) was defined as the onset temperature of the endothermic peak.

TGA Analysis: 5–10 mg of AWD sample was placed in an alumina crucible and heated from 30°C to 600°C at a rate of 10°C·min^{-1} under an air atmosphere (flow rate: 50 mL·min^{-1}). The thermogravimetric curve was recorded to analyze thermal stability and thermal decomposition process.

(a)

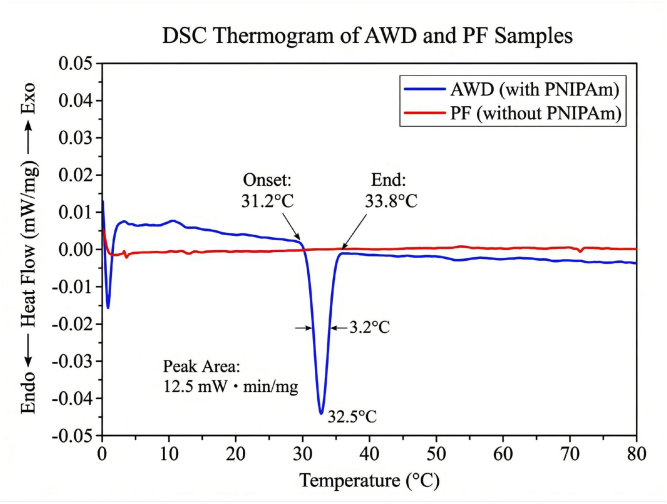

(b)

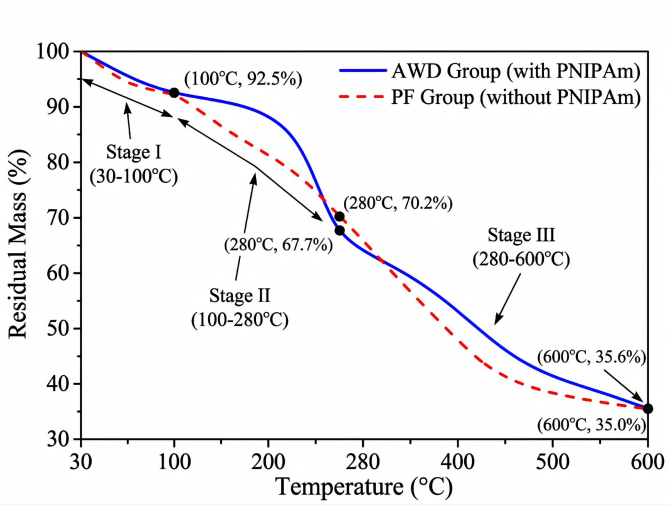

Supplementary Figure S5 Thermal performance characterization of AWD and PNIPAm-free: (a) DSC curves reveal differences in thermal responsiveness (LCST); (b) TGA curves analyze thermal decomposition behavior

AWD samples were cut into 10 mm×10 mm×1.5 mm cubes and dried in a vacuum oven at 60°C for 24 h to a constant weight (W_0). The dried samples were immersed in PBS buffer (pH 7.4) at 25°C (below LCST) and 37°C (above LCST), respectively. At predetermined time points (0.5, 1, 2, 4, 6, 8, 24 h), the samples were removed, and surface water was gently blotted with filter paper before weighing (W_t). Three parallel samples were set for each experimental group, and the swelling ratio (SR) was calculated as follows:

$$SR = (W_t - W_0) / W_0 \times 100\%$$

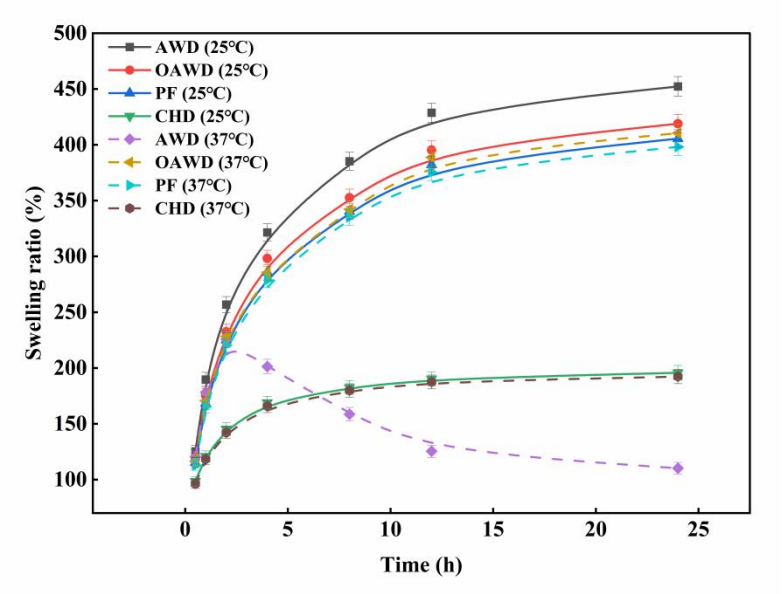

Supplementary Figure S6 Comparison of swelling rates of AWD, OAWD, PF, and CHD at 25°C/37°C

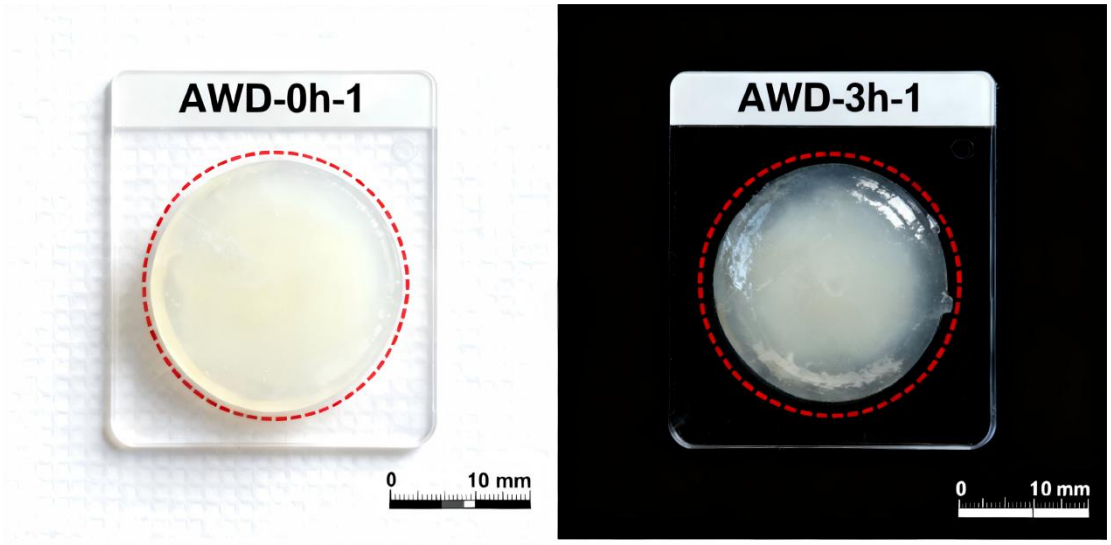

Supplementary Figure S7 Representative images of AWD before and after temperature treatment (37°C, 3 h). (A) AWD before treatment; (B) AWD after 3 h incubation at 37°C. Scale bar = 10 mm.

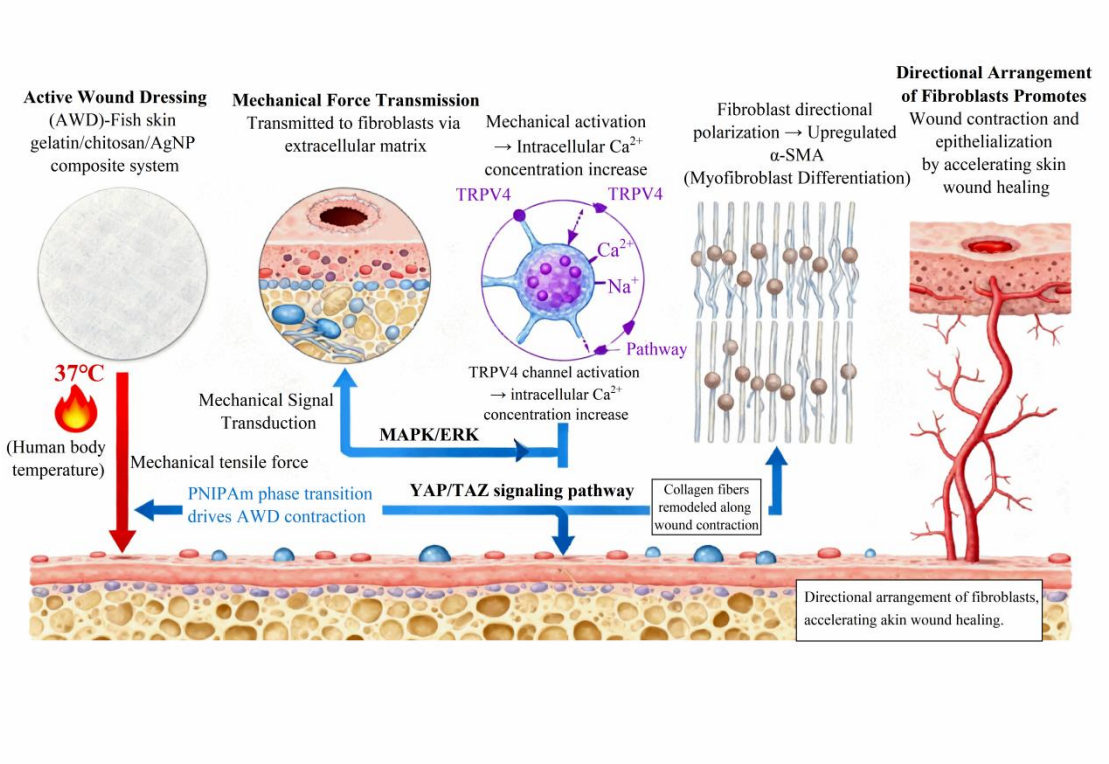

Supplementary Figure S8 Hypothesized Mechanism of Wound Healing Induced by TRPV4-activated AWD